Supplementary information for *"The critical role of policy enforcement in achieving health, air quality and climate benefits of India's clean electricity transition"*

Wei Peng, Hancheng Dai, Hao Guo, Pallav Purohit, Johannes Urpelainen, Fabian Wagner, Yazhen Wu , Hongliang Zhang*

*Corresponding author. School of International Affairs and Department of Civil and Environmental Engineering, Penn State university, weipeng@psu.edu

24 pages
14 figures
9 tables

This supplementary information includes the following contents:

1. Additional information for methods
    a. Population
    b. Baseline mortality rates
    c. CO_2 emissions from non-electricity sectors in 2015
    d. WRF-CMAQ domain
    e. Three groups of states with low, medium and high SDI
2. Additional results
    a. Share of advanced coal technologies and CO_2 emissions by coal power generation technologies
    b. Simulated $PM_{2.5}$ concentrations in 2040
    c. State-average $PM_{2.5}$ concentrations
    d. Co-control of CO_2 emissions and air pollution-related health impacts
3. Sensitivity analyses on different exposure-response functions
4. Sensitivity analyses on changing baseline mortality rate

Appendix: Introduction to the IMED|HEL model

1. Additional information on methods

1.1 Population

For 2015, the state-level population by age group is obtained from the data visualization platform of GBD India Compare[1]. We calculate the population with 5-year age intervals by dividing all-cause deaths by all-cause death rates in each state. For 2040, we use projections from the Shared Socioeconomic Pathways #2 (SSP2) gridded population data[2] and estimate state-total population by aggregating the gridded data within each state. We further assume the same age structure across the country in 2040 by applying the national-level age structure projection of SSP2 to all states.

Specifically, Table S1-3 summarizes: 1) the state-total population in 2015 and 2040, 2) age structure in 2015 by state, and 3) age structure in 2040 at the national level.

Table S1 Summary of the state-level population in 2015 and projection for 2040

GAINS-South Asia Region	States	Population (million)	
		2015	2040
INDI_ANPR	Andhra Pradesh	92.54	120.14
INDI_ASSA	Assam	34.74	41.50
INDI_BENG	West Bengal	99.47	125.60
INDI_BIHA	Bihar	118.75	131.57
INDI_CHHA	Chhattisgarh	29.26	33.59
INDI_DELH	Delhi	18.15	17.91
INDI_EHIM	North East (excl. Assam)[1]	15.89	20.08
INDI_GOA	Goa	1.48	1.74
INDI_GUJA	Gujarat	67.37	79.48
INDI_HARY	Haryana	28.29	35.52
INDI_HIPR	Himachal Pradesh	7.40	8.59
INDI_JHAR	Jharkhand	37.21	44.52
INDI_KARN	Karnataka	66.72	85.32
INDI_KERA	Kerala	35.26	46.83
INDI_MAHA	Maharashtra[2]	122.09	147.09
INDI_MAPR	Madhya Pradesh	83.03	98.61
INDI_ORIS	Orissa	46.63	59.16
INDI_PUNJ	Punjab[3]	30.27	41.48
INDI_RAJA	Rajasthan	78.01	92.06
INDI_TAMI	Tamil Nadu[4]	79.65	96.01
INDI_UTAN	Uttaranchal	11.04	12.62
INDI_UTPR	Uttar Pradesh	227.44	269.45
INDI_WHIM	Jammu and Kashmir	13.28	19.12

[1] North East region consists of 7 small north eastern states (viz. Arunachal Pradesh, Manipur, Meghalaya, Mizoram, Nagaland, Sikkim and Tripura).
[2] Including Dadra-Nagar Haveli and Daman and Diu (Union Territories - UTs)
[3] Including Chandigarh (UT)
[4] Including The Andaman and Nicobar Islands, Lakshadweep and Pondicherry (UTs)

Table S2 Summary of the age structure in Indian states, 2015

State	Sex	0-4	25-29	30-34	35-39	40-44	45-49	50-54	55-59	60-64
Andhra Pradesh	Both	8.0%	8.9%	8.5%	7.6%	6.8%	5.9%	4.8%	4.0%	3.7%
Assam	Both	10.6%	8.7%	8.2%	7.1%	6.1%	5.1%	4.0%	3.1%	2.4%
West Bengal	Both	8.2%	8.9%	8.3%	7.4%	6.7%	6.0%	5.0%	4.1%	3.3%
Bihar	Both	12.3%	7.2%	7.0%	6.2%	5.1%	4.1%	3.2%	2.8%	2.7%
Delhi	Both	8.6%	9.7%	9.3%	7.8%	6.7%	5.6%	4.5%	3.6%	3.0%
Arunachal Pradesh	Both	11.5%	8.7%	7.9%	6.8%	5.6%	4.6%	3.4%	2.4%	1.7%
Goa	Both	6.4%	8.7%	8.7%	8.6%	8.0%	7.1%	6.0%	5.2%	4.5%
Gujarat	Both	9.4%	8.8%	8.2%	7.3%	6.3%	5.5%	4.6%	3.8%	3.1%
Haryana	Both	10.4%	9.0%	8.1%	6.8%	6.0%	5.0%	4.0%	3.3%	3.0%
Himachal Pradesh	Both	7.9%	8.5%	8.3%	7.7%	6.9%	6.1%	5.2%	4.4%	3.7%
Jharkhand	Both	13.5%	8.0%	7.7%	6.5%	5.4%	4.6%	3.7%	3.1%	2.9%
Karnataka	Both	8.5%	9.4%	8.7%	7.5%	6.6%	5.7%	4.6%	3.8%	3.3%
Kerala	Both	7.6%	7.2%	7.3%	7.2%	7.2%	6.9%	6.4%	5.7%	4.9%
Maharashtra	Both	8.2%	9.2%	8.5%	7.4%	6.5%	5.6%	4.6%	3.8%	3.4%
Madhya Pradesh	Both	3.9%	8.1%	7.4%	6.5%	5.8%	4.9%	3.9%	3.0%	2.7%
Punjab	Both	8.2%	9.0%	8.4%	7.2%	6.5%	5.7%	4.7%	4.1%	3.8%
Rajasthan	Both	11.8%	8.2%	7.2%	6.3%	5.5%	4.7%	3.8%	3.0%	2.5%
Tamil Nadu	Both	8.1%	8.5%	8.5%	7.9%	7.2%	6.5%	5.5%	4.6%	3.9%
Uttar Pradesh	Both	11.9%	7.7%	6.8%	6.1%	5.3%	4.3%	3.4%	2.8%	2.6%
Jammu and Kashmir	Both	9.1%	8.8%	8.2%	0.7%	6.1%	5.1%	4.0%	3.1%	2.5%
Nagaland	Both	9.9%	8.7%	8.2%	7.0%	5.9%	4.7%	3.5%	2.6%	1.9%
Manipur	Both	9.6%	9.4%	8.6%	7.4%	6.3%	5.5%	4.6%	3.7%	2.8%
Mizoram	Both	9.7%	9.3%	8.5%	7.2%	5.9%	4.9%	4.2%	3.4%	2.4%
Tripura	Both	8.5%	9.3%	8.6%	7.5%	6.7%	5.8%	4.7%	3.7%	2.8%
Meghalaya	Both	11.0%	8.7%	7.6%	6.0%	4.9%	4.2%	3.3%	2.4%	1.8%
Sikkim	Both	7.9%	10.4%	9.6%	7.8%	6.3%	5.2%	4.2%	3.4%	2.6%
Telangana	Both	8.5%	9.5%	8.8%	7.6%	6.4%	5.2%	4.1%	3.5%	3.2%
Chhattisgarh	Both	11.2%	8.3%	7.8%	6.7%	5.9%	5.2%	4.1%	3.2%	2.7%
Odisha	Both	9.8%	8.2%	8.0%	7.0%	6.2%	5.6%	4.7%	3.9%	3.6%
Uttarakhand	Both	9.1%	8.6%	7.9%	6.7%	5.8%	5.0%	4.1%	3.5%	3.1%

Table S2 (Continuted)

State	65-69	70-74	75-79	80-84	85-89	90-94	95+	80+	> 25	> 30
Andhra Pradesh	3.0%	2.0%	1.2%	0.6%	0.3%	0.1%	0.0%	1.0%	57.4%	48.4%
Assam	1.7%	1.2%	0.9%	0.4%	0.1%	0.0%	0.0%	0.6%	49.0%	40.3%
West Bengal	2.3%	1.6%	1.1%	0.6%	0.2%	0.0%	0.0%	0.8%	55.6%	46.7%
Bihar	2.1%	1.3%	0.7%	0.4%	0.1%	0.0%	0.0%	0.6%	43.1%	35.9%
Delhi	2.1%	1.4%	1.0%	0.6%	0.2%	0.0%	0.0%	0.8%	55.5%	45.8%
Arunachal Pradesh	1.1%	0.8%	0.7%	0.4%	0.1%	0.0%	0.0%	0.5%	44.1%	35.5%
Goa	3.4%	2.4%	1.7%	1.0%	0.4%	0.1%	0.0%	1.4%	65.8%	57.1%
Gujarat	2.1%	1.6%	1.3%	0.7%	0.2%	0.1%	0.0%	1.0%	53.6%	44.8%
Haryana	2.3%	1.5%	1.0%	0.6%	0.3%	0.1%	0.0%	0.9%	51.1%	42.0%
Himachal Pradesh	2.6%	2.0%	1.5%	1.0%	0.4%	0.1%	0.0%	1.5%	58.2%	49.7%
Jharkhand	2.1%	1.3%	0.7%	0.4%	0.1%	0.0%	0.0%	0.5%	46.4%	38.4%
Karnataka	2.5%	1.8%	1.2%	0.6%	0.2%	0.1%	0.0%	0.9%	56.0%	46.6%

State	65-69	70-74	75-79	80-84	85-89	90-94	95+	80+	> 25	> 30
Kerala	3.4%	2.5%	1.9%	1.2%	0.5%	0.1%	0.0%	1.8%	62.4%	55.3%
Maharashtra	2.7%	2.0%	1.4%	0.7%	0.3%	0.1%	0.0%	1.1%	56.2%	47.0%
Madhya Pradesh	2.0%	1.5%	1.0%	0.5%	0.2%	0.0%	0.0%	0.7%	47.3%	39.2%
Punjab	2.8%	1.9%	1.3%	0.8%	0.4%	0.1%	0.0%	1.3%	56.8%	47.8%
Rajasthan	1.9%	1.4%	1.0%	0.5%	0.2%	0.0%	0.0%	0.8%	46.1%	37.9%
Tamil Nadu	2.8%	1.9%	1.3%	0.7%	0.2%	0.0%	0.0%	1.0%	59.8%	51.3%
Uttar Pradesh	2.0%	1.4%	0.9%	0.4%	0.2%	0.0%	0.0%	0.6%	43.9%	36.1%
Jammu and Kashmir	1.9%	1.5%	1.2%	0.7%	0.2%	0.1%	0.0%	1.0%	44.2%	35.3%
Nagaland	1.4%	1.1%	0.9%	0.5%	0.2%	0.0%	0.0%	0.8%	46.8%	38.1%
Manipur	1.8%	1.3%	0.9%	0.5%	0.2%	0.1%	0.0%	0.8%	53.3%	43.8%
Mizoram	1.7%	1.2%	0.9%	0.5%	0.2%	0.0%	0.0%	0.8%	50.5%	41.2%
Tripura	2.0%	1.5%	1.2%	0.7%	0.2%	0.1%	0.0%	0.9%	54.7%	45.4%
Meghalaya	1.3%	0.9%	0.7%	0.4%	0.1%	0.0%	0.0%	0.6%	42.4%	33.7%
Sikkim	1.8%	1.4%	1.1%	0.6%	0.2%	0.0%	0.0%	0.8%	54.5%	44.1%
Telangana	2.6%	1.9%	1.4%	0.7%	0.2%	0.0%	0.0%	1.0%	55.2%	45.7%
Chhattisgarh	2.1%	1.5%	1.1%	0.5%	0.2%	0.0%	0.0%	0.7%	49.4%	41.1%
Odisha	2.5%	1.8%	1.2%	0.6%	0.2%	0.0%	0.0%	0.9%	53.6%	45.4%
Uttarakhand	2.5%	1.6%	1.1%	0.6%	0.2%	0.0%	0.0%	0.9%	51.0%	42.4%

Table S3 Share of different age groups in national total population in 2040

Age	Ratio	Age	Ratio
0-4	3.6%	60-64	6.3%
5-9	3.9%	65-69	7.7%
10-14	4.3%	70-74	7.1%
15-19	4.6%	75-79	4.6%
20-24	5.0%	80-84	2.9%
25-29	5.2%	85-89	1.7%
30-34	6.0%	90-94	0.5%
35-39	6.2%	95+	0.1%
40-44	7.0%	80+	5.2%
45-49	7.6%	>25	78.6%
50-54	8.6%	>30	73.3%
55-59	7.1%	15-64	63.7%

1.2 Baseline mortality rates

In our main results, we use 2015 state-level, age- and disease-specific baseline mortality rates from GBD India Compare[1] to calculate deaths in both 2015 and 2040. However, baseline mortality rates often decrease over time with growing income levels and better healthcare systems. We hence conduct a sensitivity test by updating 2040 baseline mortality rates based on projections from GBD Foresight[3] (see the health results presented in Section 4). Note that we choose not to change baseline mortality rates in our main results due to a few limitations of GBD Foresight projection data, including: i) the projected mortality rate is only available at the national level; ii) it does not provide projected $PM_{2.5}$ concentrations to help understand natural death rates, i.e., death rates when all other risk factors except for $PM_{2.5}$ exposure are considered. As such, we calculate the state-level baseline mortality rates for 2040 by multiplying the 2040 national-level mortality rate from GBD Foresight by state-specific scale factors calculated as the ratio of the state-level to national-level mortality rate in 2015.

The 2015 and 2040 baseline mortality rates used in this study are summarized in Table S4. The age- and disease-specific mortality rates are projected to decline from 2015-2040. However, due to the effect of population aging, for some diseases, the all-age mortality rates increase from 2015 to 2040. Similarly, all-cause baseline mortality rates for the adult population (30+) are projected to be slightly higher in 2040 than in 2015.

Table S4 Summary of state-level baseline mortality data used in this study*

Region	Lung cancer (All age)		LRI (All age)		COPD (All age)		Diabetes mellitus type2 (All age)	
Year	**2015**	**2040**	**2015**	**2040**	**2015**	**2040**	**2015**	**2040**
INDI_ANPR	5.3	11.4	25.5	22.9	58.5	81.9	14.5	29.1
INDI_ASSA	5.2	11.1	43.9	39.4	56.8	79.5	10.3	20.6
INDI_BENG	7.7	16.6	27.9	25.0	55.6	77.8	7.6	15.2
INDI_BIHA	4.7	10.1	45.3	40.6	49.1	68.7	7.6	15.3
INDI_CHHA	5.6	11.9	55.1	49.5	56.5	79.1	13.2	26.6
INDI_DELH	7.7	16.5	21.0	18.8	26.4	37.0	13.0	26.1
INDI_EHIM	8.4	18.0	38.4	34.5	42.6	59.6	9.9	20.0
INDI_GOA	6.4	13.7	26.4	23.7	41.2	57.6	27.5	55.3
INDI_GUJA	5.5	11.7	30.1	27.0	74.3	103.9	10.9	21.9
INDI_HARY	5.8	12.4	33.7	30.3	78.6	109.9	12.4	24.9
INDI_HIPR	7.1	15.2	29.6	26.5	112.9	157.9	8.3	16.6
INDI_JHAR	3.8	8.1	37.2	33.4	42.6	59.6	9.8	19.7
INDI_KARN	6.3	13.6	28.1	25.2	82.8	115.9	22.9	46.0
INDI_KERA	15.1	32.5	21.9	19.6	64.1	89.7	25.2	50.6
INDI_MAHA	5.3	11.4	28.7	25.7	63.1	88.3	13.0	26.2
INDI_MAPR	5.1	10.9	51.0	45.7	74.1	103.7	9.5	19.1
INDI_ORIS	5.4	11.5	48.4	43.4	30.7	42.9	9.4	18.8
INDI_PUNJ	5.4	11.5	26.4	23.7	33.4	46.7	23.5	47.2
INDI_RAJA	4.8	10.3	59.0	52.9	107.9	151.1	4.5	9.1

INDI_TAMI	6.4	13.6	26.4	23.7	44.9	62.8	40.8	82.1
INDI_UTAN	7.5	16.2	42.3	37.9	103.6	145.0	13.4	26.9
INDI_UTPR	4.5	9.6	58.3	52.3	89.8	125.6	7.9	15.9
INDI_WHIM	7.4	15.9	31.6	28.3	67.0	93.8	6.0	12.1

Table S4 (Continued)

	Stroke (Older than 25)		**IHD (Older than 25)**		**All Causes (Older than 30)**	
Region	**2015**	**2040**	**2015**	**2040**	**2015**	**2040**
INDI_ANPR	87.1	66.1	232.7	197.3	1366.6	1368.5
INDI_ASSA	146.1	110.8	90.1	76.4	1375.6	1377.5
INDI_BENG	190.6	144.6	183.5	155.6	1255.0	1256.7
INDI_BIHA	76.3	57.9	154.7	131.2	1263.2	1265.0
INDI_CHHA	210.1	159.4	171.6	145.5	1813.1	1815.6
INDI_DELH	42.9	32.6	172.5	146.3	941.3	942.6
INDI_EHIM	103.7	78.7	102.0	86.5	1192.4	1194.1
INDI_GOA	82.4	62.5	203.3	172.4	1034.5	1035.9
INDI_GUJA	57.9	43.9	228.8	194.1	1289.6	1291.4
INDI_HARY	56.5	42.8	245.4	208.1	1433.4	1435.4
INDI_HIPR	49.3	37.4	166.8	141.4	1236.5	1238.3
INDI_JHAR	75.8	57.5	158.4	134.3	1310.5	1312.3
INDI_KARN	105.1	79.7	267.0	226.4	1590.2	1592.4
INDI_KERA	124.1	94.1	293.5	248.9	1388.1	1390.0
INDI_MAHA	91.8	69.7	209.1	177.3	1181.1	1182.8
INDI_MAPR	107.7	81.7	186.0	157.7	1531.4	1533.5
INDI_ORIS	148.1	112.3	88.9	75.4	1457.6	1459.6
INDI_PUNJ	57.1	43.3	303.0	257.0	1213.6	1215.3
INDI_RAJA	59.3	45.0	140.1	118.8	1391.1	1393.0
INDI_TAMI	70.0	53.1	310.0	262.9	1453.4	1455.4
INDI_UTAN	62.6	47.4	187.4	158.9	1495.4	1497.4
INDI_UTPR	58.1	44.1	156.8	133.0	1591.2	1593.4
INDI_WHIM	61.9	47.0	192.6	163.3	1220.1	1221.8

*Note: For stroke, IHD and all-cause mortality, the mortality data for population with age "older than 25" or "older than 30" are calculated based on original mortality and population data with 5-year intervals.

1.3 CO_2 emissions from non-electricity sectors in 2015

We use the GAINS-South Asia model to estimate state-level CO_2 emisisons in 2015 for the electricity and non-electricity sectors. National total CO_2 emissions are estimated to be 2275 million tons. The power sector contributes to 47% of all-sector CO_2 emissions, followed by the industry sector (35%), transportation sector (12%) and residential sector (7%).

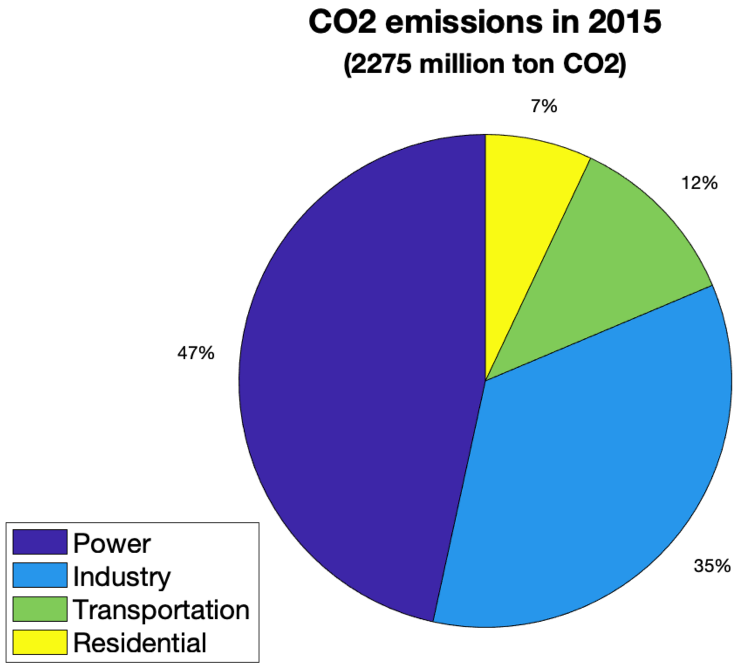

Figure S1. CO_2 emissions in 2015 by sector, estimated using GAINS-South Asia.

1.4 WRF-CMAQ simulation domain

Here we show the WRF-CMAQ simulation domain over India. The spatial resolution is 36 × 36 km^2. The color scale in Figure S2 is based on the population density in 2015 for each grid box[4].

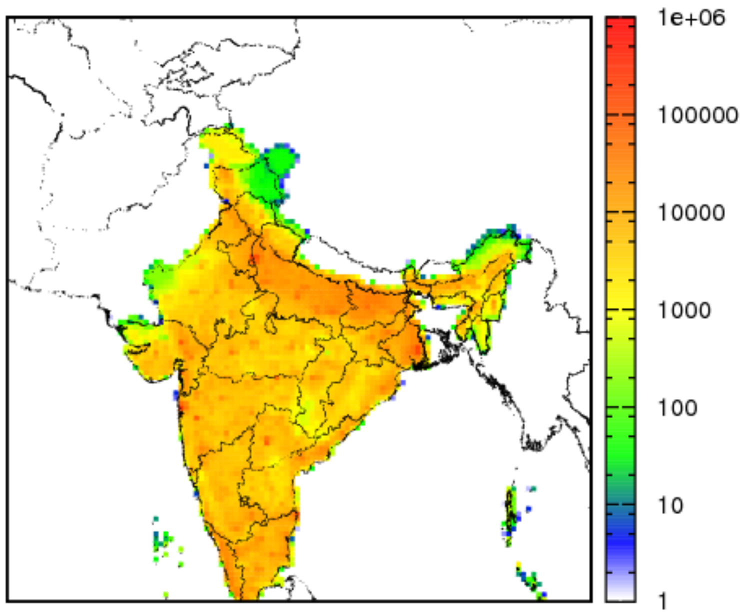

Figure S2. Design of 36 × 36 km^2 domain over India with the color scale representing the population density in 2015 in each grid (original figure see supplementary materials in Guo et al. 2018[5]).

1.5 Three groups of states with a low, medium, and high socio-demographic index (SDI)

We summarize in Table S5 and Figure S3 the states with a low, medium and high socio-demographic index, following the categorization in Balakrishnan 2019[6]. The SDI is developed based on a variety of factors, including per-capita income, mean education level and total fertility rate.

Table S5 States with low-, medium- and high-SDI

Low-SDI states	Bihar, Madhya Pradesh, Jharkhand, Uttar Pradesh, Rajasthan, Chhattisgarh, Odisha, Assam
Medium-SDI states	Andhra Pradesh, West Bengal, Tripura, Arunachal Pradesh, Meghalaya, Karnataka, Telangana, Gujarat, Manipur, Jammu and Kashmir, Haryana
High-SDI states	Uttarakhand, Tamil Nadu, Mizoram, Maharashtra, Punjab, Sikkim, Nagaland, Himachal Pradesh, Union Territories (excluding Delhi), Kerala, Delhi, Goa

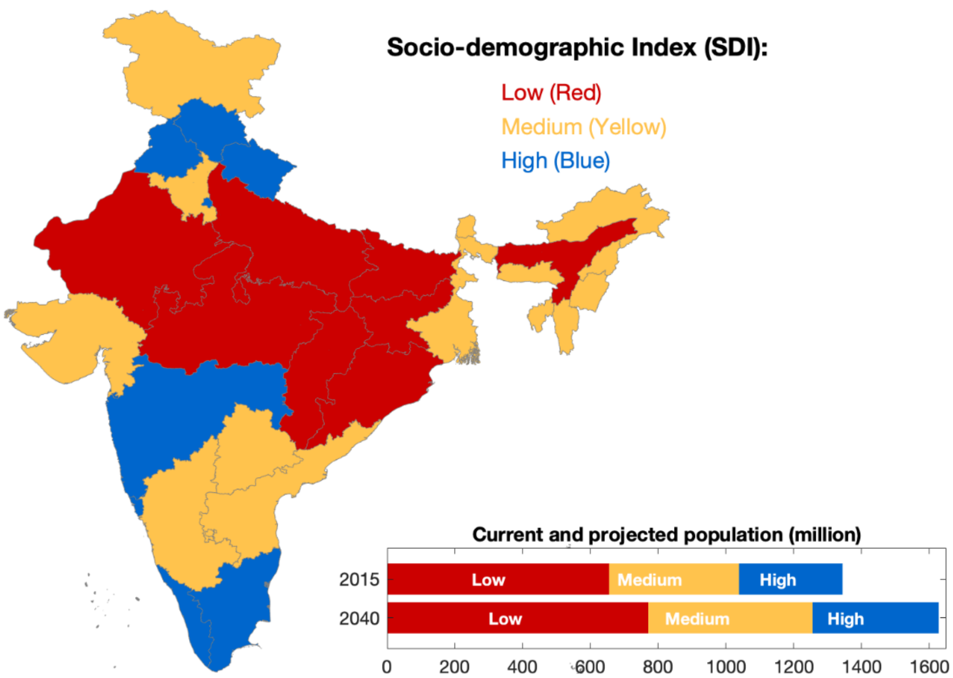

Figure S3. States with low (red), medium (yellow) and high (blue) socio-demographic index. The inserted figure on the bottom right shows each type of states' shares in the national total population in 2015 and 2040 (based on data in Table S1).

2. Additional results

2.1 Electricity generation and CO_2 emissions by coal power generation technologies

We present electricity generation and CO_2 emissions by different coal plant types in WEO-CLE, BAU-CLE and AMB-CLE (Figure S4 and S5). Note that the fuel mix and technology choices in WEO-DEL and WEO-FRO are the same as in WEO-CLE. Since we do not consider the efficiency penalty to operate end-of-control devices, the CO_2 emissions in WEO-DEL and WEO-FRO are also the same as those in WEO-CLE.

As the total amount of supercritical and ultra-supercritical coal power generation gradually increases over time (blue bars in Figure S4), associated CO_2 emissions also increase substantially from 2015 to 2040 across all three scenarios (blue bars in Figure S5). Since BAU-CLE and AMB-CLE allow for the addition of new subcritical units, these two scenarios lead to a large increase in CO_2 emissions from subcritical units (orange and red bars) from 2015 to 2022. Due to these new additions in BAU-CLE and AMB-CLE and the long lifetime of coal units, by 2040 the generation and associated CO_2 emissions from subcritical units are greater than they were in 2015, and lower than they were in 2022. In contrast, the WEO-CLE scenario assumes successful implementation of policies to increase the efficiency of newly built coal-fired power plants. It hence projects a noticeable decrease in power generation and associated CO_2 emissions from subcritical units between 2020 to 2040. This is because no new subcritical units are added after 2015 and CO_2 emissions only come from existing subcritical plants that operate until the end of their lifetime.

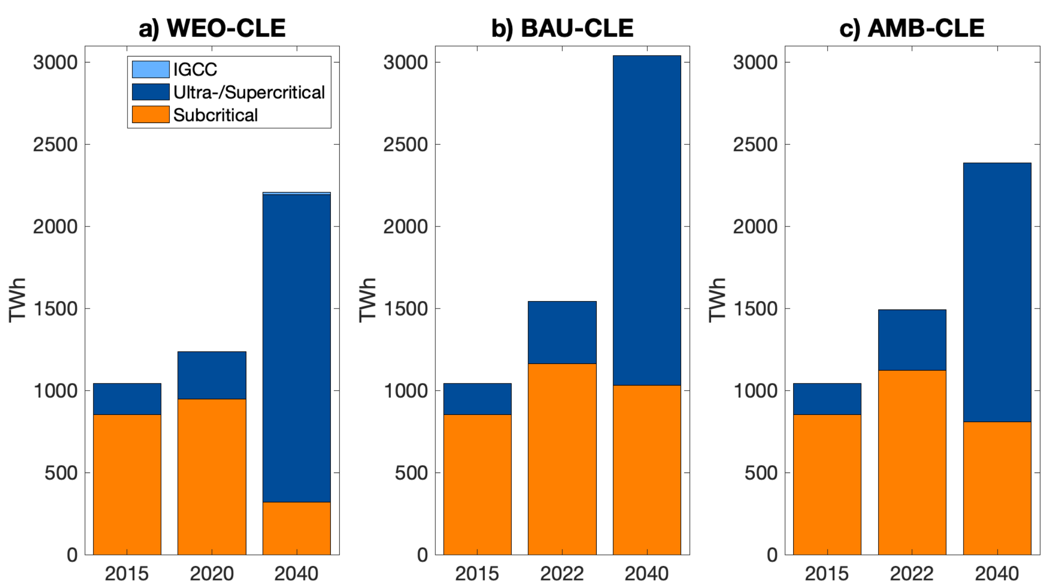

Figure S4. Coal power generation by plant type in: a) WEO-CLE, b) BAU-CLE and c) AMB-CLE scenario.

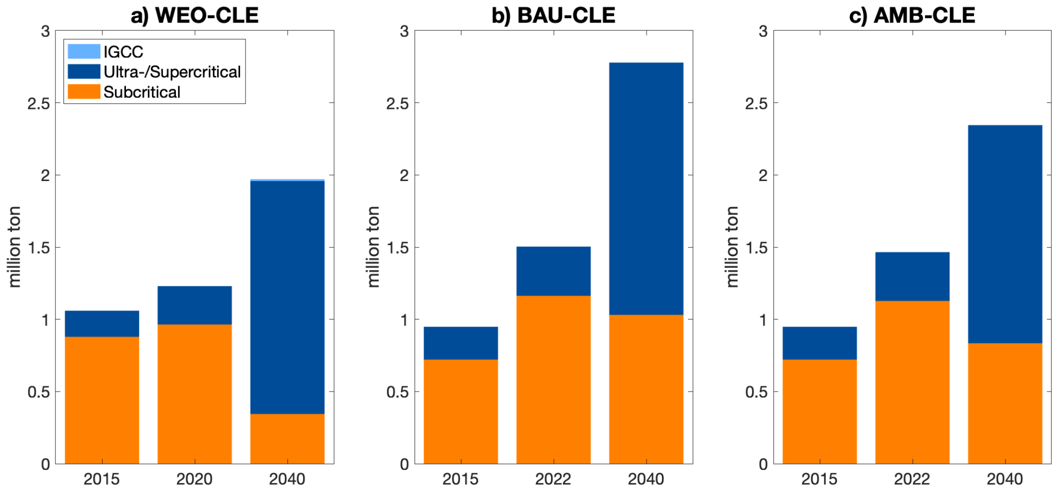

Figure S5. CO_2 emissions by coal power generation technologies in a) WEO-CLE, b) BAU-CLE and c) AMB-CLE scenario.

2.2 Simulated $PM_{2.5}$ concentrations in 2040

Here we present annual mean $PM_{2.5}$ concentrations for each of the five scenarios in 2040. Given the significant variations across different regions in India, the relative differences across scenarios are difficult to see using the color scale in Figure S6 that covers the range for absolute concentrations. Thus in the main text, we present the differences between scenarios in Figure 3b.

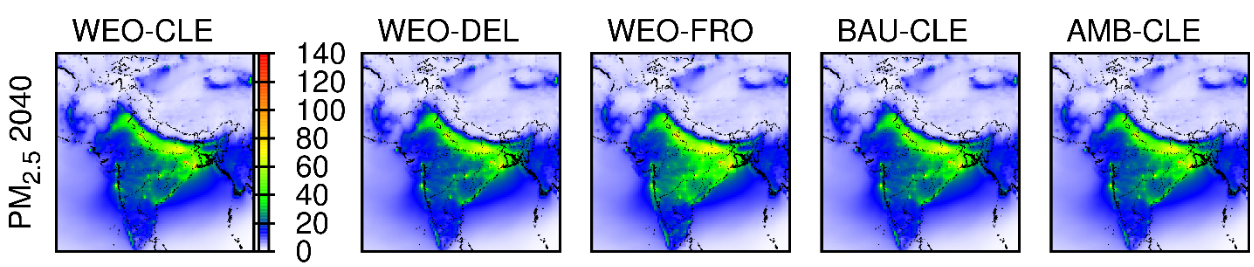

Figure S6. Spatial distribution of annual mean ambient $PM_{2.5}$ concentrations (unit: $\mu g/m^3$) in 2040. The annual mean concentrations are estimated by taking the average of monthly mean concentrations for four representative months (i.e., January, April, July and October).

2.3 State-average $PM_{2.5}$ concentrations

We highlight two observations. First, in WEO-CLE, the annual mean $PM_{2.5}$ concentration is similar in 2015 and 2040, both in terms of scale and spatial distribution. Second, comparing other scenarios to WEO-CLE, the annual mean $PM_{2.5}$ concentration increases by 0-5 $\mu g/m^3$ throughout the country in WEO-DEL, BAU-CLE and AMB-CLE, while the pollution level increases by more than

$5 \mu g/m^3$ in most provinces in WEO-FRO. As a result, we also observe the greatest increase in $PM_{2.5}$-related deaths in WEO-FRO, with the highest death toll observed in north and central India.

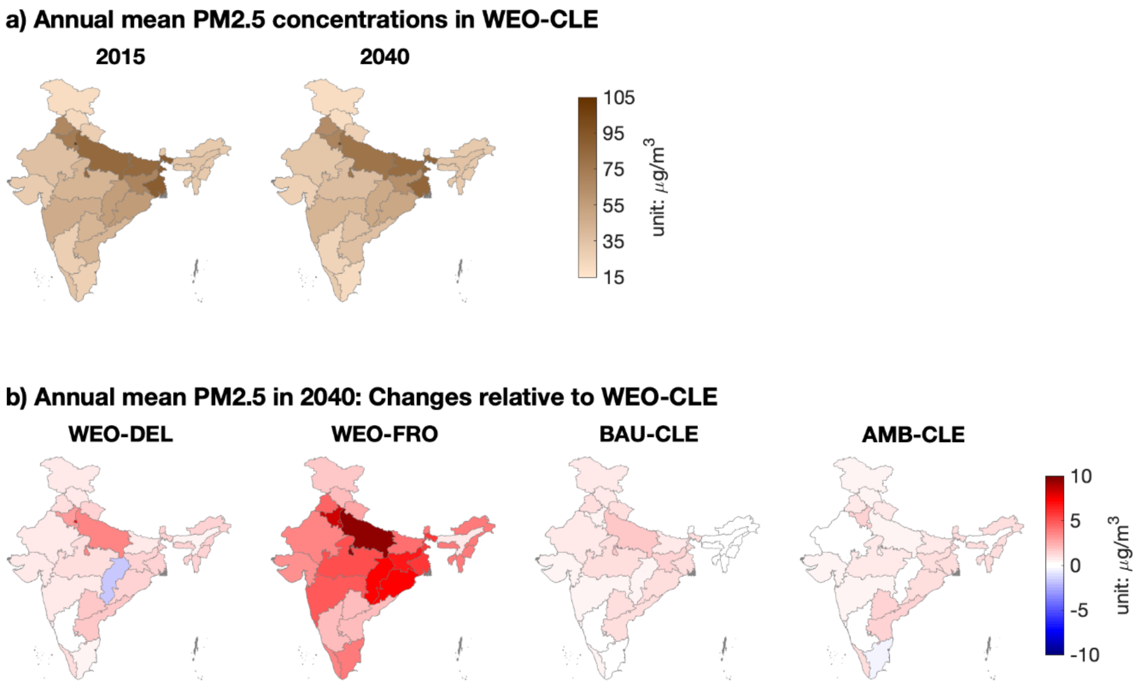

Figure S7. State-averaged annual mean $PM_{2.5}$ concentrations: a) in WEO-CLE: 2015 and 2040; b) in 2040: changes in each scenario relative to WEO-CLE.

2.4 Co-control of CO_2 emissions and air pollution-related health impacts

Given the dual challenge of simultaneously curbing CO_2 emissions and air pollution, we provide a comprehensive perspective by comparing the percentage change in CO_2 and air pollution impacts. Since air pollution impacts are affected by all-sector emissions, we present the 2015 to 2040 changes as: i) *all-sector* CO_2 emissions (i.e., 2040 power sector emissions plus 2015 non-power emissions); ii) total $PM_{2.5}$-related deaths as a result of *all-sector* air pollutant emissions. Non-power emissions are kept at 2015 levels and estimated using the GAINS-South Asia model with proper validation (Supplementary Figure S1).

Nationally, for the five scenarios examined, we find much greater cross-scenario variations in all-sector CO_2 impacts (i.e., 40-80% higher than 2015 across 5 scenarios) than total air pollution impacts (i.e., 50-57% higher than 2015 across 5 scenarios). This is because while CO_2 impacts are directly affected by the amount of fossil fuel generation in the future, some level of air pollution control always exists (even in the delayed or frozen air pollution policy scenarios) since some measures are already being taken today.

With huge subnational heterogeneity in socioeconomic development levels, we further demonstrate unequal impacts across states with a low, medium or high socio-demographic index (SDI) (see Supplementary Table S5 and Figure S3 for categorization of low-, medium- and high-SDI states). The low-, medium-, and high-SDI states represent 47%, 29% and 24% of the total population in 2015, and we assume that this population pattern largely persists in 2040. This subnational perspective is relevant not only for addressing environmental justice concerns, but also for policy considerations regarding the enforcement of policies given the cross-state variations in institutional capacity.

For changes in $PM_{2.5}$-related deaths from 2015 to 2040, across all five scenarios, we observe the smallest percentage increase in high-SDI states and the largest percentage increase in medium-SDI states. These cross-region differences are driven by a variety of socioeconomic and policy factors, including cross-state variations in pollution levels, age structure, and baseline mortality rates. For CO_2 emissions, since energy pathways are the key to determine CO_2 impacts, the largest CO_2 increase occurs in medium-SDI states under the WEO energy projection, while the largest increase occurs in high-SDI states under the BAU and AMB energy projections. Such differences are driven by the different geographic patterns of renewable energy deployment at the subnational level as projected in WEO and BAU/AMB.

Despite the differences across states with different SDIs, our main findings remain robust in all three groups of states, namely: i) limited enforcement of air pollution policies results in more health damage from air pollution but has a limited impact on CO_2 emissions; and ii) limited enforcement of energy policies leads to significantly more CO_2 emissions, but results in only slightly more $PM_{2.5}$-related deaths.

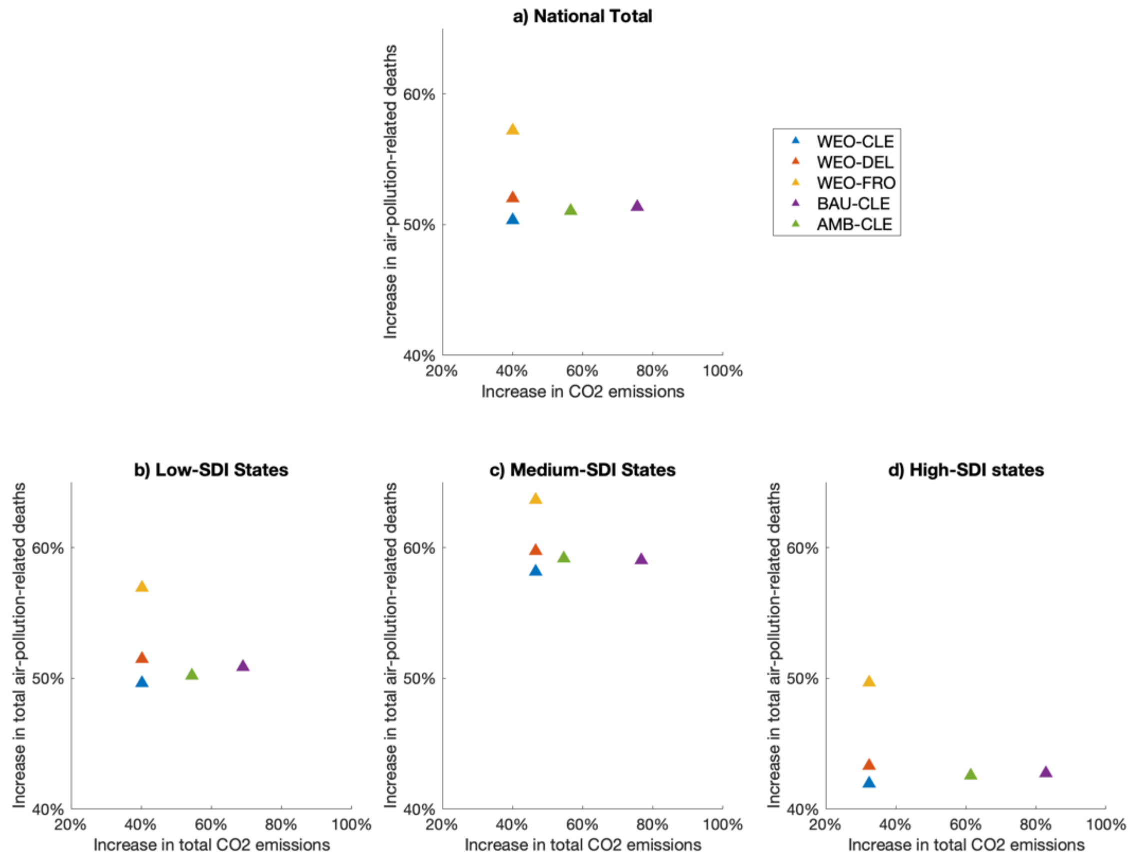

Figure S8. Increases in all-sector CO_2 emissions and total $PM_{2.5}$-related deaths in 2040 relative to 2015 for: a) National total; b) Low-SDI states; c) Medium-SDI states; d) High-SDI states.

3. Sensitivity analyses on different exposure-response functions

The choice of the exposure-response functions (ERFs) often affects the health impact assessment results in a substantial way [7–9]. We use non-linear relative risk (RR) functions from GBD for six diseases (ischemic heart disease (IHD), stroke, chronic obstructive pulmonary disease (COPD), lung cancer (LC), lower respiratory tract infections (LRI) and diabetes) in the main results, which are denoted as integrated exposure-response (IER) functions. Here, we further consider: a) GEMM: Mortality from five diseases (i.e., COPD, IHD, Lung Cancer, Stroke, LRI) based on the exposure-response functions from the Global Exposure Mortality Model (GEMM)[10], and b) Log-linear: All-cause mortality estimated using the log-linear relative risk function based on Pope et al. (2002)[11]. Note that IER and GEMM functions consider specific $PM_{2.5}$-related diseases, whereas the log-linear function targets all-cause mortality. This assumption makes GEMM results more directly comparable with IER results than log-linear results. Furthermore, non-linear RR functions are more consistent with recent epidemiological evidence that the marginal mortality risks decrease with increasing $PM_{2.5}$ concentrations at high levels. Detailed methods are presented in Table S9.

3.1 National total mortality

In most scenarios, national total $PM_{2.5}$-related deaths are greater when using the GEMM or log-linear functions than when using the IER functions (Figure S9 and Table S6). Quantitatively, in 2015, premature mortality is estimated to be 0.86 million (95% CI: 0.55-1.13 million), 1.33 million (0.97-1.60 million) and 1.65 million (0.62-2.66 million), when using IER, GEMM and log-linear functions, respectively. In the 2040 scenarios, the central estimates of the national total mortality increase to 1.29-1.35 million based on the IER functions, 2.27-2.39 million based on GEMM functions, and 2.51-2.81 million based on the log-linear functions. However, under all ERFs, the lowest mortalities are observed in the WEO-CLE scenario and the highest are observed in the WEO-FRO scenario.

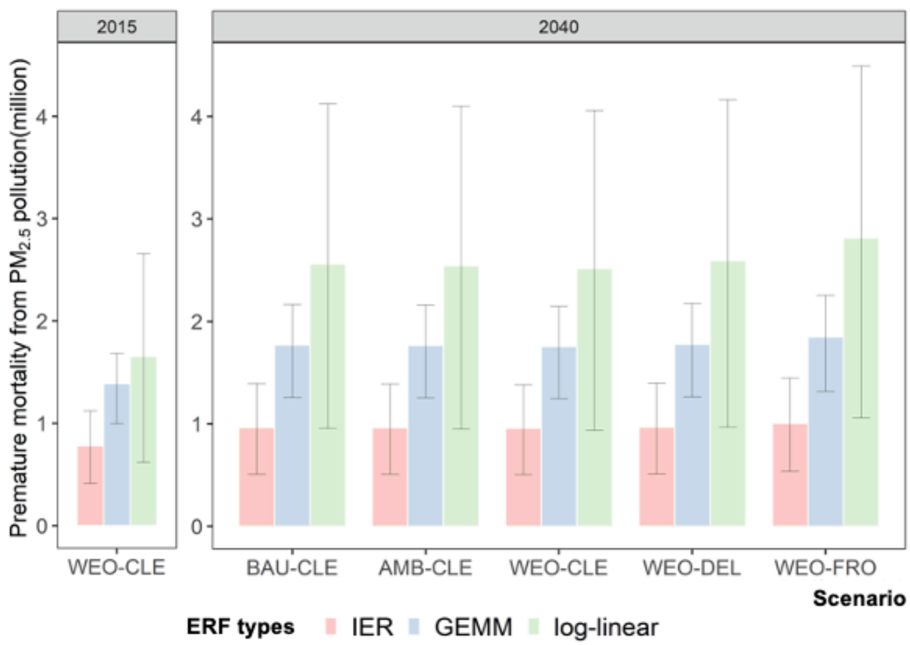

Figure S9 Sensitivity of the total mortality in India under three different exposure-response functions. Note: IER: six causes; GEMM: five causes; log-linear: all-cause.

Table S6. National total mortality estimated using different ERFs (unit: million)

		IER (six diseases)			GEMM (five diseases)			log-linear (all-cause)		
Year	**Scenario**	**central**	**low**	**high**	**central**	**low**	**high**	**central**	**low**	**high**
2015	/	0.857	0.555	1.129	1.325	0.968	1.602	1.653	0.619	2.655
2040	WEO-CLE	1.289	0.807	1.740	2.272	1.692	2.732	2.511	0.936	4.052
	WEO-FRO	1.348	0.855	1.806	2.394	1.787	2.870	2.811	1.058	4.487
	WEO-DEL	1.303	0.819	1.756	2.300	1.715	2.764	2.587	0.967	4.160
	AMB-CLE	1.295	0.812	1.747	2.285	1.702	2.747	2.542	0.948	4.097

	BAU-CLE	1.298	0.814	1.750	2.290	1.706	2.753	2.557	0.954	4.118

Note: The “central” estimates are the central estimates from the ERF; the “low” and “high” estimates represent the 95% confidence intervals of mortality estimates considering the uncertainty range of the ERF parameters.

The shape of the ERF functions is likely the main driver of higher mortality estimates under GEMM when compared to IER. GEMM integrates the results of many up-to-date large-scale epidemiological cohort studies across the world, including one Chinese male cohort study with high long-term ambient $PM_{2.5}$ exposure level. As such, GEMM provides more up-to-date estimates for RR at high $PM_{2.5}$ ranges, resulting in higher RR than IER[10].

To provide a quantitative perspective, in Figure S10 we plot the RR curves and the population attributable fraction (PAF) as a function of rising $PM_{2.5}$ concentration for IER and GEMM (Figure S9). We choose to plot IHD and COPD, one as an example of age-specific RR (IHD) that is available from GEMM and the other as an example of aggregated RR for populations older than 25. It is clear that the relative risks and PAFs are significantly higher under the GEMM functions than in the IER functions.

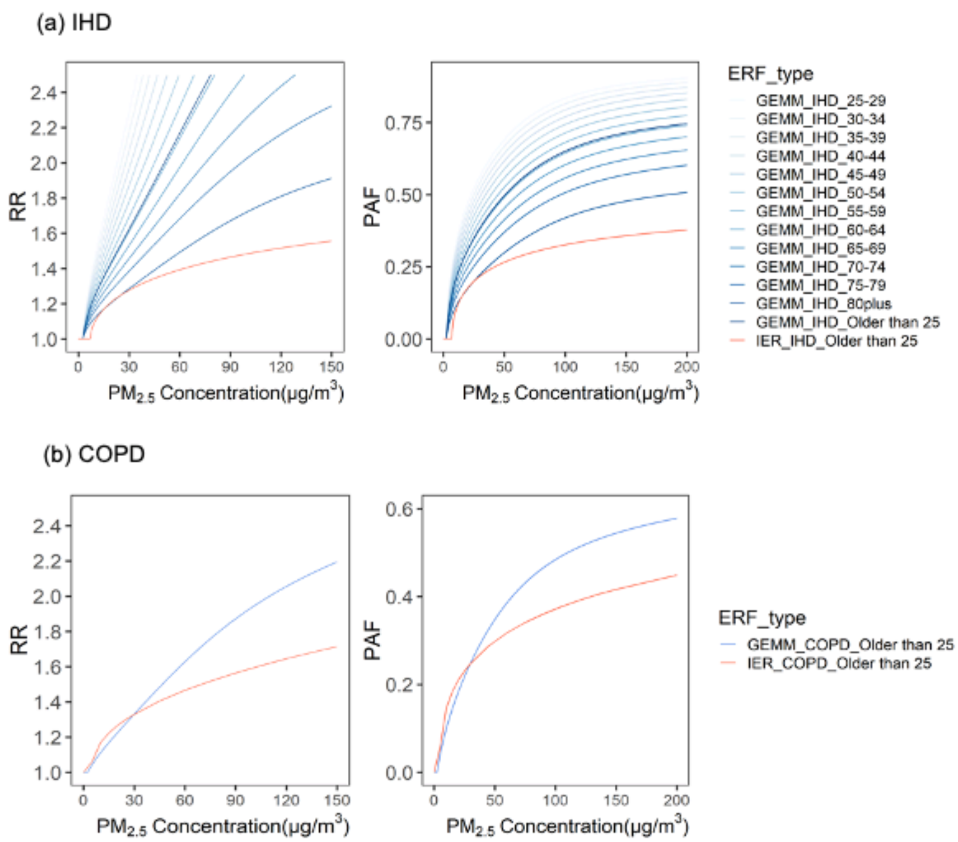

Figure S10. Relative risk and population attributable fraction of (a) IHD (b) COPD mortality as a function of increasing $PM_{2.5}$ concentration, for different ERFs.

However, the choice of ERFs does not affect our main finding that unsucecessful implementation of energy or air pollution control policies would lead to more deaths, although it does affect the absolute and percentage differences across scenarios (Figure S11). Regardless of the choice of ERFs, in 2040, the lowest deaths occur under the WEO-CLE scenario and the highest deaths occur in the WEO-FRO scenario. The differences across scenarios are smallest under the IER functions. This implies that our main results are likely conservative estimates for $PM_{2.5}$-related deaths, and hence conservative estimates for the benefits of successful policy implementation on human health.

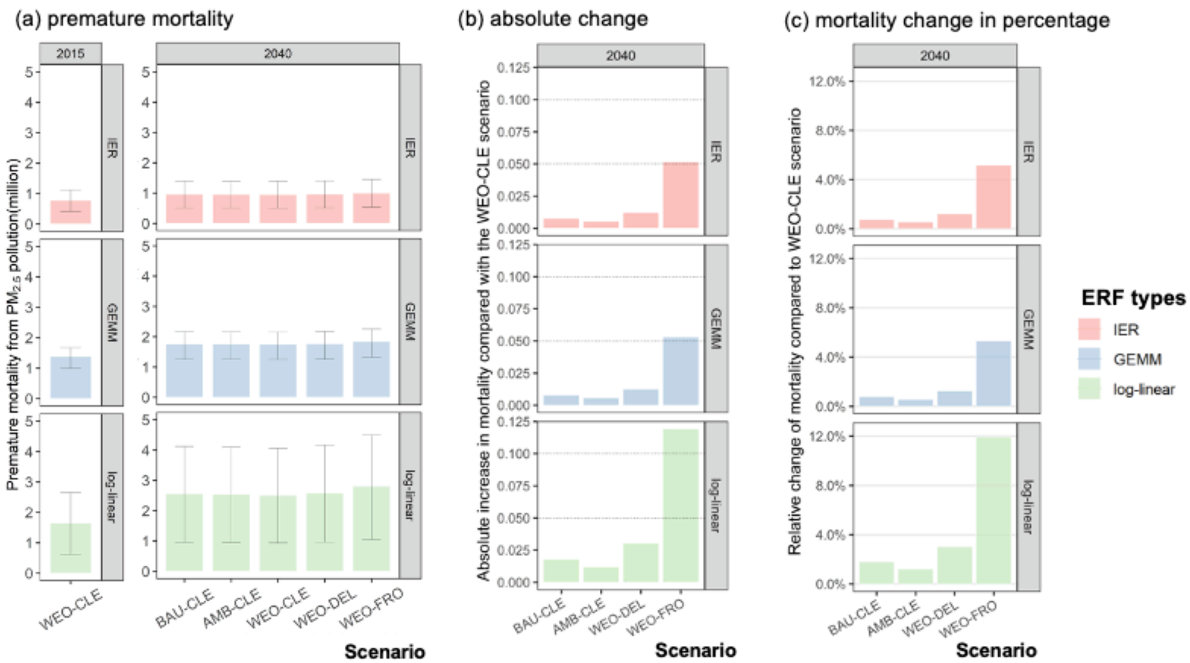

Figure S11. $PM_{2.5}$-related premature mortality in India based on different ERFs: (a) total $PM_{2.5}$-related premature mortality in all scenarios, (b) absolute change in 2040 relative to WEO-CLE, and (c) relative change in 2040 relative to WEO-CLE.

3.2 State-level mortality

Differences due to the choice of ERFs vary across states (Figure S12 and Table S7). In most states, the estimated mortality using the IER function is smaller than when using the log-linear or GEMM functions. However, in some states the IER results can be higher than the log-linear results. For states with concentration levels higher than 40μg/m^3 in 2040 under the WEO-CLE scenario (including INDI_DELH, INDI_BENG, INDI_BIHA, INDI_UTPR, INDI_HARY, INDI_PUNJ, INDI_JHAR, INDI_ORIS, and INDI_CHHA), we find that applying the log-linear functions always yields the highest deaths, followed by GEMM and then IER. This pattern could be explained by: (i) log-linear RR functions are applied to all-cause mortality that includes more diseases; and (ii) the RR increases rapidly at high $PM_{2.5}$ concentration ranges, especially for GEMM functions.

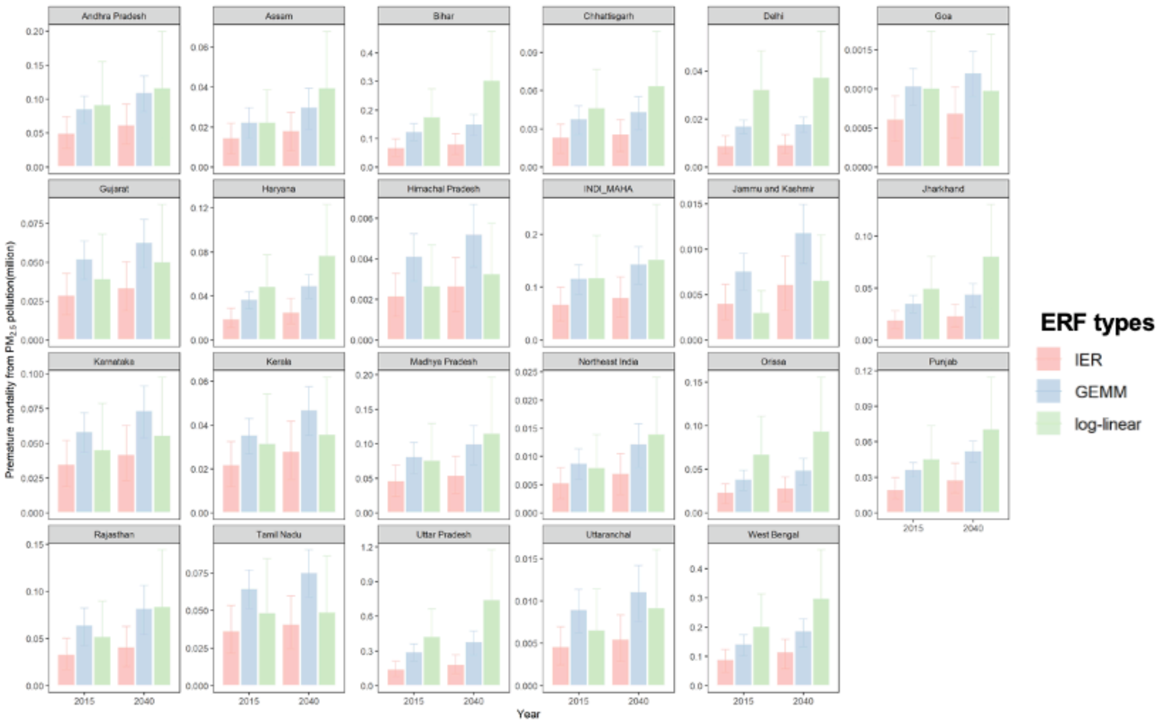

Figure S12. $PM_{2.5}$-related premature mortality in Indian states, under the WEO-CLE scenario
Note: INDI_MAHA is the abbreviation for the region Maharashtra-Dadra-Nagar Haveli-Daman-Diu. Same for the other figures.

Table S7. $PM_{2.5}$ level and $PM_{2.5}$-related deaths in 2040 for WEO-CLE, by state*

Region	**$PM_{2.5}$** ($\mu g/m^3$)	**$PM_{2.5}$-related premature mortality** (million)		
		IER (six diseases)	**GEMM (five disease)**	**Log-linear (all-cause)**
India	33.02	1.29	2.27	2.51
INDI_ANPR	32.45	0.08	0.14	0.12
INDI_ASSA	79.77	0.03	0.04	0.04
INDI_BENG	76.84	0.12	0.27	0.30
INDI_BIHA	45.16	0.11	0.20	0.30
INDI_CHHA	95.17	0.03	0.06	0.06
INDI_DELH	28.62	0.01	0.03	0.04
INDI_EHIM	27.34	0.01	0.02	0.01
INDI_GOA	25.57	0.00	0.00	0.00
INDI_GUJA	63.17	0.05	0.08	0.05
INDI_HARY	19.57	0.03	0.07	0.08
INDI_HIPR	57.88	0.00	0.01	0.00
INDI_JHAR	22.96	0.03	0.06	0.08
INDI_KARN	27.56	0.07	0.10	0.06

Region	$PM_{2.5}$ (μg/m^3)	**$PM_{2.5}$-related premature mortality** (million)		
		IER (six diseases)	**GEMM (five disease)**	**Log-linear (all-cause)**
INDI_KERA	38.81	0.03	0.05	0.04
INDI_MAHA	34.91	0.10	0.18	0.15
INDI_MAPR	46.56	0.08	0.13	0.12
INDI_ORIS	58.88	0.03	0.06	0.09
INDI_PUNJ	31.10	0.04	0.07	0.07
INDI_RAJA	20.99	0.07	0.10	0.08
INDI_TAMI	25.49	0.07	0.10	0.05
INDI_UTAN	72.82	0.01	0.01	0.01
INDI_UTPR	18.75	0.26	0.48	0.75
INDI_WHIM	33.02	0.01	0.01	0.01

*Note: (1) Only the central estimates are shown; (2) "India" results are calculated by adding up the results of all the states.

Similar to national-level results, different ERFs lead to different additional deaths due to policy failures (Figure S13). However, the choice of ERF does not affect the relative size of deaths across policy failure scenarios: the WEO-FRO scenario always leads to the highest $PM_{2.5}$-related premature mortality, while mortality under the three other policy failure scenarios is similar (i.e., ~1% more deaths than WEO-CLE scenario under IER and GEMM functions for most states, and ~5% more deaths under the log-linear functions).

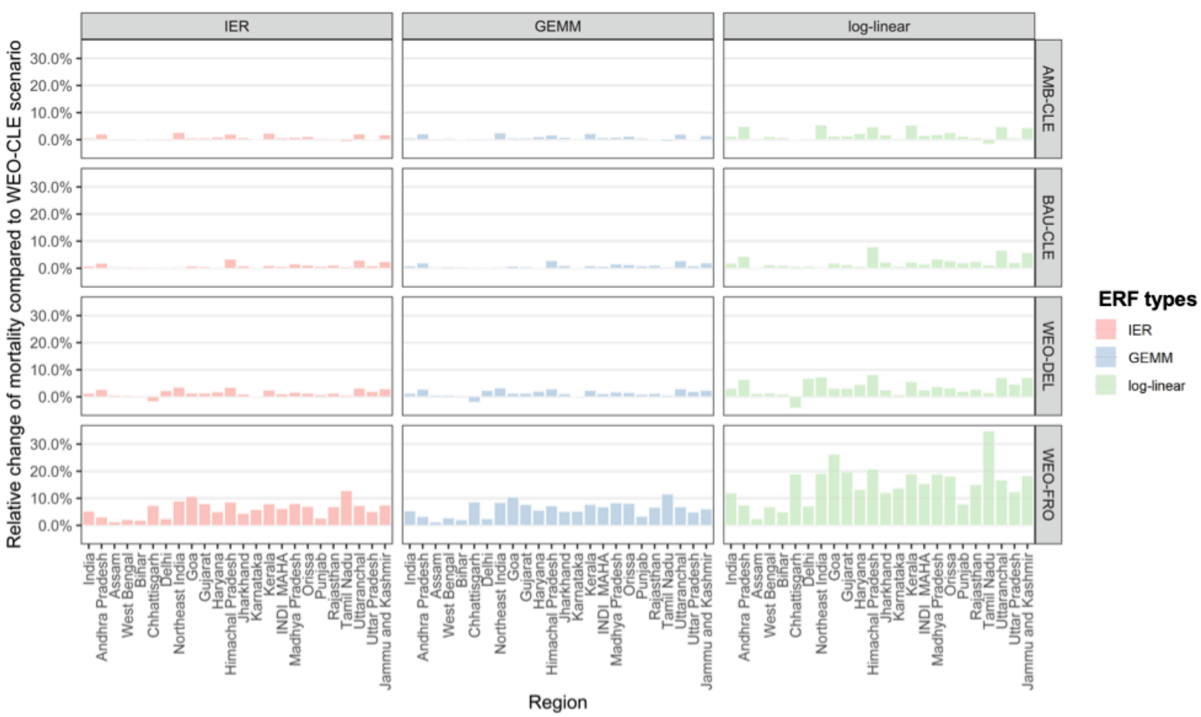

Figure S13. Differences in state-level mortality in 2040 compared with WEO-CLE scenario, under the three ERFs.

4. Sensitivity analyses on baseline mortality rates

Here we consider changing baseline mortality rates from 2015 to 2040 based on projections from GBD Foresight and current cross-state variations (see Table S4). For IER and GEMM results, we find lower 2040 $PM_{2.5}$-related deaths in all scenarios when applying projected 2040 age- and disease-specific baseline mortality rates than applying 2015 rates. The percentage decreases are greater under GEMM than IER. Log-linear functions, in comparison, only consider all-cause mortality for the adult population aged 30 years or above. With population aging, the all-age baseline mortality rate is projected to increase slightly in 2040 when compared to 2015. As such, when log-linear functions are used, we find a minimal increase in the death estimates using 2040 baseline mortality rates instead of the 2015 ones.

However, the changes in $PM_{2.5}$-related deaths in the policy failure scenarios when compared to WEO-CLE are not significantly affected by the choice of baseline mortality rates. For instance, with RR functions from IER (i.e., our main results), the WEO-DEL, WEO-FRO, BAU-CLE, AMB-CLE scenarios lead to 1.2%, 4.8%, 0.7% and 0.5% more deaths than WEO-CLE in 2040 when using projected 2040 baseline mortality rates (Figure S14). Those numbers are only marginally different from results using 2015 baseline mortality rates, i.e, 1.1%, 4.6%, 0.7% and 0.5%, respectively. This finding remains robust when GEMM or log-linear RR functions are used.

Table S8. National $PM_{2.5}$-related deaths in 2040 calculated using the 2015 (Main) and 2040 baseline mortality rates (Updated). Unit: Million deaths.

		WEO-CLE			**WEO-DEL**			**WEO-FRO**		
IER	**Main**	1.29	0.81	1.74	1.30	0.82	1.76	1.35	0.85	1.81
	Updated	1.18	0.75	1.55	1.19	0.76	1.56	1.23	0.80	1.61
	% Diff	*-9%*	*-7%*	*-11%*	*-9%*	*-7%*	*-11%*	*-9%*	*-7%*	*-11%*
GEMM	**Main**	2.27	1.69	2.73	2.30	1.71	2.76	2.39	1.79	2.87
	Updated	1.61	1.15	1.98	1.63	1.16	2.00	1.70	1.21	2.07
	% Diff	*-29%*	*-32%*	*-28%*	*-29%*	*-32%*	*-28%*	*-29%*	*-32%*	*-28%*
Log-linear	**Main**	2.51	0.94	4.05	2.59	0.97	4.16	2.81	1.06	4.49
	Updated	2.51	0.94	4.06	2.59	0.97	4.17	2.81	1.06	4.49
	% Diff	*0.1%*	*0.1%*	*0.1%*	*0.1%*	*0.1%*	*0.1%*	*0.1%*	*0.1%*	*0.1%*

Table S8 (continued)

		BAU-CLE			**AMB-CLE**		
IER	**Main**	1.30	0.81	1.75	1.29	0.81	1.75
	Updated	1.18	0.76	1.56	1.18	0.75	1.55
	% Diff	-9%	-7%	-11%	-9%	-7%	-11%
GEMM	**Main**	2.29	1.71	2.75	2.28	1.70	2.75
	Updated	1.62	1.16	1.99	1.62	1.15	1.99

	% Diff	-29%	-32%	-28%	-29%	-32%	-28%
Log-linear	**Main**	2.56	0.95	4.12	2.54	0.95	4.10
	Updated	2.56	0.96	4.12	2.55	0.95	4.10
	% Diff	0.1%	0.1%	0.1%	0.1%	0.1%	0.1%

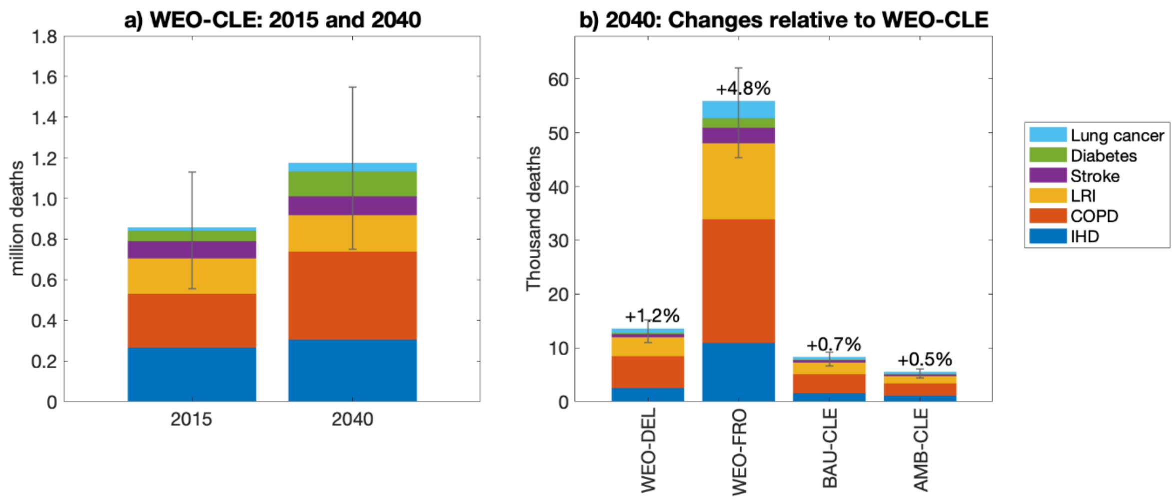

Figure S14. National total $PM_{2.5}$-related deaths with changing baseline mortality rates from 2015 to 2040: a) for 2015 and 2040 in WEO-CLE, and b) changes in other scenarios relative to WEO-CLE in 2040. Here the estimates are based on the IER relative risk functions, consistent with our main results.

Appendix: Introduction to the IMED|HEL model

In this study, the sensitivity analyses on alternative exposure-response functions are conducted using the IMED|HEL model. It assesses the health impacts by using different $PM_{2.5}$ exposure-response functions (in this study, log-linear, non-linear IER, and non-linear GEMM functions) to estimate the relative risk of $PM_{2.5}$ pollution and excess mortality under certain scenarios. By comparing the health assessment results of different scenarios, the model can be used to analyze the human health benefits of air pollution control policies and energy policies. The IMED|HEL model is compatible with both gridded and regional exposure data, and can be used to estimate the health impacts at gridded, regional and national levels.

The detailed underlying methods in the IMED|HEL model to estimate the $PM_{2.5}$-related health impacts are presented in Table S9. More information about the IMED|HEL model can be found in prior work published using this model [12–15] and the online documentation [16].

Table S9 Methods to estimate the health impacts using the IMED|HEL model

Health endpoint	Methods
Mortality	The general method for mortality risk assessment is the same as that in the main text, but with some differences in the formula for different ERFs. The excess mortality ($\Delta Mort$) is estimated using the following formula: $$\Delta Mort = \sum_e \frac{(RR(C)_e - 1)}{RR(C)_e} \cdot I \cdot Population$$ Where *I* is the reported death rate for a specific disease, and $RR(C)_e$ is the relative risk of mortality for disease e under the $PM_{2.5}$ pollution level *C*: $$RR(C)_e = \begin{cases} 1 & ,when\ C - C_0 \leq 0 \\ e^{\beta_e(C-C_0)} & ,when\ C - C_0 > 0\ \ (log-linear\ model) \\ 1 + \alpha_e\,[1 - e^{-\gamma_e(C-C_0)^{\delta}}] & ,when\ C - C_0 > 0\ \ (IER\ model) \\ e^{[\theta_e log(\frac{C-C_0}{\alpha_e}+1)]/[1+e^{-\frac{C-C_0-\mu}{v}}]} & ,when\ C - C_0 > 0\ \ (GEMM\ model) \end{cases}$$ Note that the threshold concentrations, C_0, are different in the three ERFs. For log-linear function we take 10μg/m^3, for IER function it ranges between 2.4-5.8μg/m^3, and for the GEMM function the threshold is 2.4μg/m^3. For the log-linear model, we only consider the all-cause mortality (i.e. there is only one kind of mortality endpoint —"all-cause") in adults aged 30 or above. In this study, the IMED|HEL model is used for estimating the mortality under the linear and GEMM functions to be compared with the IER results in the main text.

Reference

(1) Indian Council of Medical Research; Public Health Foundation of India; Institute for Health Metrics and Evaluation. GBD India Compare Data Visualization. *Available from http://vizhub.healthdata.org/gbd-compare/india* **2017**.

(2) Jones, B.; O'Neill, B. C. Global Population Projection Grids Based on Shared Socioeconomic Pathways (SSPs), 2010-2100. NASA Socioeconomic Data and Applications Center (SEDAC): Palisades, NY 2017.

(3) Institute for Health Metrics and Evaluation (IHME). GBD Foresight. *Available from: https://vizhub.healthdata.org/gbd-foresight/* **2018**.

(4) UNITED NATIONS; DESA / POPULATION DIVISION. The World Population 2015. **2015**.

(5) Guo, H.; Kota, S. H.; Chen, K.; Sahu, S. K.; Hu, J.; Ying, Q.; Wang, Y.; Zhang, H. Source Contributions and Potential Reductions to Health Effects of Particulate Matter in India. *Atmos. Chem. Phys.* **2018**, *18* (20), 15219–15229. https://doi.org/10.5194/acp-18-15219-2018.

(6) Balakrishnan, K.; Dey, S.; Gupta, T.; Dhaliwal, R. S.; Brauer, M.; Cohen, A. J.; Stanaway, J. D.; Beig, G.; Joshi, T. K.; Aggarwal, A. N.; Sabde, Y.; Sadhu, H.; Frostad, J.; Causey, K.; Godwin, W.; Shukla, D. K.; Kumar, G. A.; Varghese, C. M.; Muraleedharan, P.; Agrawal, A.; Anjana, R. M.; Bhansali, A.; Bhardwaj, D.; Burkart, K.; Cercy, K.; Chakma, J. K.; Chowdhury, S.; Christopher, D. J.; Dutta, E.; Furtado, M.; Ghosh, S.; Ghoshal, A. G.; Glenn, S. D.; Guleria, R.; Gupta, R.; Jeemon, P.; Kant, R.; Kant, S.; Kaur, T.; Koul, P. A.; Krish, V.; Krishna, B.; Larson, S. L.; Madhipatla, K.; Mahesh, P. A.; Mohan, V.; Mukhopadhyay, S.; Mutreja, P.; Naik, N.; Nair, S.; Nguyen, G.; Odell, C. M.; Pandian, J. D.; Prabhakaran, D.; Prabhakaran, P.; Roy, A.; Salvi, S.; Sambandam, S.; Saraf, D.; Sharma, M.; Shrivastava, A.; Singh, V.; Tandon, N.; Thomas, N. J.; Torre, A.; Xavier, D.; Yadav, G.; Singh, S.; Shekhar, C.; Vos, T.; Dandona, R.; Reddy, K. S.; Lim, S. S.; Murray, C. J. L.; Venkatesh, S.; Dandona, L. The Impact of Air Pollution on Deaths, Disease Burden, and Life Expectancy across the States of India: The Global Burden of Disease Study 2017. *The Lancet Planetary Health* **2019**, *3* (1), e26–e39. https://doi.org/10.1016/S2542-5196(18)30261-4.

(7) Lin, J.; Du, M.; Chen, L.; Feng, K.; Liu, Y.; V. Martin, R.; Wang, J.; Ni, R.; Zhao, Y.; Kong, H.; Weng, H.; Liu, M.; van Donkelaar, A.; Liu, Q.; Hubacek, K. Carbon and Health Implications of Trade Restrictions. *Nature Communications* **2019**, *10* (1), 4947. https://doi.org/10.1038/s41467-019-12890-3.

(8) Dedoussi, I. C.; Eastham, S. D.; Monier, E.; Barrett, S. R. H. Premature Mortality Related to United States Cross-State Air Pollution. *Nature* **2020**, *578* (7794), 261–265. https://doi.org/10.1038/s41586-020-1983-8.

(9) Lelieveld, J.; Evans, J. S.; Fnais, M.; Giannadaki, D.; Pozzer, A. The Contribution of Outdoor Air Pollution Sources to Premature Mortality on a Global Scale. *Nature* **2015**, *525*, 367.

(10) Burnett, R.; Chen, H.; Szyszkowicz, M.; Fann, N.; Hubbell, B.; Pope, C. A.; Apte, J. S.; Brauer, M.; Cohen, A.; Weichenthal, S.; Coggins, J.; Di, Q.; Brunekreef, B.; Frostad, J.; Lim, S. S.; Kan, H.; Walker, K. D.; Thurston, G. D.; Hayes, R. B.; Lim, C. C.; Turner, M. C.; Jerrett, M.; Krewski, D.; Gapstur, S. M.; Diver, W. R.; Ostro, B.; Goldberg, D.; Crouse, D. L.; Martin, R. V.; Peters, P.; Pinault, L.; Tjepkema, M.; van Donkelaar, A.; Villeneuve, P. J.; Miller, A. B.; Yin, P.; Zhou, M.; Wang, L.; Janssen, N. A. H.; Marra, M.; Atkinson, R. W.; Tsang, H.; Quoc Thach, T.; Cannon, J. B.; Allen, R. T.; Hart, J. E.; Laden, F.; Cesaroni, G.; Forastiere, F.; Weinmayr, G.; Jaensch, A.; Nagel, G.; Concin, H.; Spadaro, J. V. Global Estimates of Mortality Associated with Long-Term Exposure to Outdoor Fine Particulate Matter. *Proc Natl Acad Sci USA* **2018**, *115* (38), 9592. https://doi.org/10.1073/pnas.1803222115.

(11) Pope III, C. A.; Burnett, R. T.; Thun, M. J.; Calle, E. E.; Krewski, D.; Ito, K.; Thurston, G. D. Lung Cancer, Cardiopulmonary Mortality, and Long-Term Exposure to Fine Particulate Air Pollution. *JAMA* **2002**, *287* (9), 1132–1141. https://doi.org/10.1001/jama.287.9.1132.

(12) Xie, Y.; Dai, H.; Xu, X.; Fujimori, S.; Hasegawa, T.; Yi, K.; Masui, T.; Kurata, G. Co-Benefits of Climate Mitigation on Air Quality and Human Health in Asian Countries. *Environment International* **2018**, *119*, 309–318. https://doi.org/10.1016/j.envint.2018.07.008.

(13) Xie, Y.; Dai, H.; Dong, H.; Hanaoka, T.; Masui, T. Economic Impacts from PM2.5 Pollution-Related Health Effects in China: A Provincial-Level Analysis. *Environ. Sci. Technol.* **2016**, *50* (9), 4836–4843. https://doi.org/10.1021/acs.est.5b05576.

(14) Kim, S. E.; Xie, Y.; Dai, H.; Fujimori, S.; Hijioka, Y.; Honda, Y.; Hashizume, M.; Masui, T.; Hasegawa, T.; Xu, X.; Yi, K.; Kim, H. Air Quality Co-Benefits from Climate Mitigation for Human Health in South Korea. *Environment International* **2020**, *136*, 105507. https://doi.org/10.1016/j.envint.2020.105507.

(15) Xie, Y.; Dai, H.; Zhang, Y.; Wu, Y.; Hanaoka, T.; Masui, T. Comparison of Health and Economic Impacts of PM2.5 and Ozone Pollution in China. *Environment International* **2019**, *130*, 104881. https://doi.org/10.1016/j.envint.2019.05.075.

(16) Laboratory of Energy & Environmental Economics and Policy. IMED|HEL Model Introduction. *http://scholar.pku.edu.cn/hanchengdai/imedhel*.